Anal Bioanal Chem (2012) 403:697–706
DOI 10.1007/s00216-012-5899-5

PAPER IN FOREFRONT

Electron spray ionization mass spectrometry and 2D ^{31}P NMR for monitoring ^{18}O/^{16}O isotope exchange and turnover rates of metabolic oligophosphates

Emirhan Nemutlu · Nenad Juranic · Song Zhang · Lawrence E. Ward · Tumpa Dutta · K. Sreekumaran Nair · Andre Terzic · Slobodan Macura · Petras P. Dzeja

Received: 5 January 2012 / Revised: 22 February 2012 / Accepted: 24 February 2012 / Published online: 18 March 2012

Abstract A new method was here developed for the determination of ^{18}O-labeling ratios in metabolic oligophosphates, such as ATP, at different phosphoryl moieties (α-, β-, and γ-ATP) using sensitive and rapid electrospray ionization mass spectrometry (ESI-MS). The ESI-MS-based method for monitoring of ^{18}O/^{16}O exchange was validated with gas chromatography–mass spectrometry and 2D ^{31}P NMR correlation spectroscopy, the current standard methods in labeling studies. Significant correlation was found between isotopomer selective 2D ^{31}P NMR spectroscopy and isotopomer less selective ESI-MS method. Results demonstrate that ESI-MS provides a robust analytical platform for simultaneous determination of levels, ^{18}O-labeling kinetics and turnover rates of α-, β-, and γ-phosphoryls in ATP molecule. Such method is advantageous for large scale dynamic phosphometabolomic profiling of metabolic networks and acquiring information on the status of probed cellular energetic system.

Keywords ^{18}O isotope labeling · ESI-MS · ^{31}P NMR · ATP · Energy metabolism · Phosphotransfer networks

Abbreviations

AA	Amino acids
FFA	Free fatty acids
G3P	Glycerol 3-phosphate
NTP	Nucleoside triphosphate

Introduction

Comprehensive characterization of metabolic networks and their response to functional load requires quantitative knowledge of complete sets of metabolites, their concentrations and turnover rates [1–5]. Such information enables deduction of intracellular fluxes and dynamic rearrangements in metabolic network modules determining metabolic phenotypes [6–12]. Indeed, metabolites and signaling molecules may display significant changes in turnover rates without noticeable changes in respective concentrations [9, 13–17]. In tracking metabolite turnover rates and performing fluxomic analysis of metabolic networks, stable isotope tracers such as ^{13}C, ^{18}O, and ^{15}N have been widely used [10–12, 17–24]. Among them, ^{18}O isotope has been useful due to its ability to determine

E. Nemutlu · S. Zhang · A. Terzic · P. P. Dzeja (✉)
Division of Cardiovascular Diseases, Department of Medicine,
Mayo Clinic,
Rochester, MN 55905, USA
e-mail: dzeja.petras@mayo.edu

N. Juranic · S. Macura
Department of Biochemistry and Molecular Biology, Mayo Clinic,
Rochester, MN 55905, USA

N. Juranic · S. Macura
Analytical NMR Core Facility, Mayo Clinic,
Rochester, MN 55905, USA

L. E. Ward · T. Dutta · K. S. Nair
CTSA Metabolomic Core Facility, Mayo Clinic,
Rochester, MN 55905, USA

T. Dutta · K. S. Nair
Division of Endocrinology and Endocrine Research Unit,
Mayo Clinic,
Rochester, MN 55905, USA

E. Nemutlu (✉)
Department of Analytical Chemistry, Faculty of Pharmacy,
University of Hacettepe,
06100 Ankara, Turkey
e-mail: enemutlu@hacettepe.edu.tr

phosphoryl-containing metabolite turnover rates and cellular energetic fluxes through phosphotransfer and signal transduction networks [9, 15, 23, 25–32]. Phosphate-containing metabolites play a dominant role in cellular life [33]. Most of these metabolites are highly polar and their separation and analysis especially of oligophosphates represent a challenge.

The ^{18}O-labeling methodology is based on incorporation of the ^{18}O atom from $H_2{}^{18}O$ into inorganic phosphate (P_i) during ATP hydrolysis and subsequent distribution of ^{18}O-labeled phosphoryls among phosphate-carrying molecules in metabolic networks [9, 26, 27]. Incorporation of ^{18}O-stable isotopes into oligophosphates reflect turnover rates of different phosphoryl moieties and thus its quantification offers a tool to reveal unique information regarding respective enzyme's activities [9, 23, 25–29, 34]. For instance, the efficiency of intracellular energy transfer in intact cells/tissues catalyzed by adenylate kinase, ATP synthase, and ATPase can be deduced from γ- and β-phosphoryl-labeling ratio within the ATP molecule [27] while changes in α-phosphoryl of ATP labeling in response adenine nucleotide synthesis de novo [35]. Yet, the activity of other enzymes such as pyrophosphokinase and nucleotidyltransferases [9, 36, 37] can be monitored only if more subtle analysis is introduced which can differentiate labeling of peripheral versus bridging oxygens in oligophosphates [38].

The incorporation ratio of ^{18}O isotope into oligophosphates containing metabolites can be determined either from ^{31}P NMR spectra, or by gas chromatography–mass spectrometry (GC-MS). GC-MS is a more sensitive method but requires prior metabolite separation, enzymatic transfer of each phosphoryl moiety to glycerol, derivatization and analysis of ^{18}O/^{16}O ratios in glycerol 3-phosphate (G3P) [9, 23, 31, 32, 35]. The advantage of ^{18}O-assisted ^{31}P NMR spectroscopy is that it permits non-destructive quantification of ^{18}O-labeling ratios of multiple metabolite phosphoryls in a single run; however, compared with GC-MS, it is less sensitive and thus requires a larger amount of sample and a extended analysis time [9, 27].

The goal of this work was to apply relatively insensitive, but isotopomer-selective *J*-decoupled ^{31}P NMR 2D chemical shift correlation spectroscopy to verify the more sensitive, but isotopomer nonselective, electrospray ionization mass spectrometry (ESI-MS) method. After verification of ESI-MS method for ^{18}O-labeling of ATP at different phosphoryl moiety, identical ATP samples were analyzed with both ESI-MS and GC-MS methods to compare the accuracy and sensitivity of ESI-MS. Results demonstrate that ESI-MS provides a suitable analytical platform for simultaneous analysis of ^{18}O/^{16}O exchange in different phosphoryl moieties of oligophosphates, and therefore can be used for determination of phosphoryl turnovers in nucleotide triphosphates involved in different metabolic processes.

Materials and methods

^{18}O-labeling of ATP samples

Enzymatic reactions involved in ^{18}O-stable isotope metabolic labeling of ATP molecule at different phosphoryl moieties The oxygen exchange between phosphate and $H_2[^{18}O]$ does not occur readily in nature and equilibrium is very slow [39]. Exchange of oxygens in orthophosphate requires use of enzymatic reactions [40]. When tissues or cells are exposed to media containing a known percentage (20–30%) of ^{18}O, $H_2{}^{18}O$ rapidly equilibrates with cellular water and ^{18}O is incorporated into phosphoryls of ATP proportionally to the rate of enzymatic reactions involved (Fig. 1). First, ^{18}O is incorporated into P_i during each act of ATP hydrolysis by cellular ATPases; subsequent γ-ATP ^{18}O-labeling reflects the activity of ATPsynthase regenerating nascent ATP molecules, while β-ADP/ATP ^{18}O-labeling is exclusively produced by the adenylate kinase catalyzed reaction coupled with ATPsynthase. Labeling of ATP α-phosphoryls is produced by

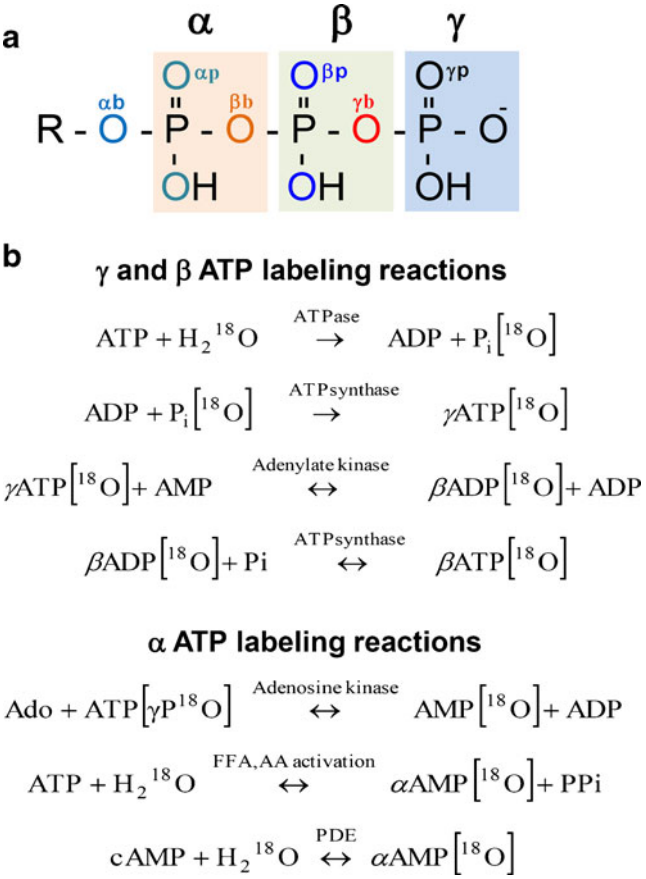

Fig. 1 Differential isotopic ^{18}O/^{16}O substitutions in ATP molecule phosphoryls (**a**). Oxygen tags: *αb* alpha bridge, *αp* alpha peripheral, *βb* beta bridge, *βp* beta peripheral, *γb* gamma bridge, *γp* gamma peripheral. Enzymatic reactions involved in ^{18}O enrichment of ATP α-, β-, and γ-phosphoryls (**b**). *FFA* free fatty acids, *AA* amino acids, *PDE* phosphodiesterase

adenosine kinase reaction in adenine nucleotide synthesis de novo while changes in α-ATP labeling in response to stress or fat/protein load can be induced by phosphodiesterase reaction and cAMP signaling or by FFA and amino acid activation [9, 23, 34].

Heart perfusion and ^{18}O phosphoryl labeling Hearts from heparinized (50 U, ip) and anesthetized (75 mg/kg pentobarbital sodium, ip) mouse or rat were excised and retrogradely perfused with a 95 % O_2–5 % CO_2-saturated Krebs–Henseleit (K-H) solution (in mM—118 NaCl, 5.3 KCl, 2.0 $CaCl_2$, 19 $NaHCO_3$, 1.2 $MgSO_4$, 11.0 glucose, and 0.5 EDTA; 37K-H°C) at a perfusion pressure of 70 mmHg. Hearts were paced at 500 beats/min for mouse and 250 beats/min for rat. Hearts were perfused for 30 min with K-H solution and then subjected to labeling with K-H solution including 30 % $H_2[^{18}O]$ 30 or 60 s for mice and 10 min for rat, were then immediately freeze-clamped [27, 28]. Frozen hearts were pulverized under liquid N_2, and extracted in a solution containing 0.6 M $HClO_4$ and 1 mM EDTA. Extracts were neutralized with 2 M $KHCO_3$ and used to determine ^{18}O incorporation into metabolite phosphoryls.

ATP purification Labeled ATP from perfused heart extracts were purified with HPLC using a Mono Q HR 5/5 ion-exchange column (Pharmacia Biotech) and 1 M triethylammonium bicarbonate buffer (pH 8.8, adjusted with CO_2) gradient elution (0.5–90 % within 25 min) at 1 mL/min flow rate [9]. The ATP fractions (around 30 min) were collected and dried out using vacuum centrifugation (SpeedVac, Savant) and reconstituted with 100 μL water.

2D ^{31}P NMR spectroscopy

The 283-MHz ^{31}P NMR spectra were recorded on a 700-MHz Avance spectrometer (Spectrospin, Billerica, MA) using an X-channel of indirect detection broadband probe for direct ^{31}P observation. The pulse sequence used for ^{31}P chemical shift correlations of $^{18}O/^{16}O$ isotopic effects and corresponding experimental details were described previously [38]. The $^{18}O/^{16}O$ isotope effects are readily visible in high-resolution ^{31}P NMR by ^{18}O-induced ^{31}P chemical shifts (Fig. 2a). However, due to scalar couplings in polyphosphates ^{31}P NMR lines are already split into doublets/triplets and $^{18}O/^{16}O$ isotope exchange effects which introduce additional lines in the ^{31}P NMR spectrum creating a complex pattern of overlapping peaks (Fig. 2a). A better separation of isotopomers was enabled herein by the *J*-decoupled ^{31}P-^{31}P 2D correlated spectroscopy improved ^{31}P spectra of polyphosphates by eliminating the line splitting due to the scalar coupling, and more importantly, by sorting out correlations between different isotopologues (Fig. 2b) [38].

GC-MS

The details of ^{18}O-labeling at different phosphoryl moieties have been reported earlier [32]. Briefly, the γ-, β-, and α-phosphoryl of purified ATP were transferred to glycerol in a series of enzymatic and chemical reactions (Fig. 2c). First the γ-phosphoryl of ATP was transferred to glycerol by glycerokinase, and then the β-phosphoryl of ATP was transferred to glycerol by a combined catalytic action of adenylate kinase and glycerokinase. Finally the α-phosphoryl of ATP was transferred to glycerol by AMP-deaminase and Smith degradation. Samples that contained phosphoryls of γ-, β-, and α-ATP as G3P, were derivatizated using *N*-methyl-*N*-trimethyl-silyltrifluoroacetamide+1% trimethylchlorosilane (MSTFA+1% TMCS; Thermo Fisher) mixture. The ^{18}O enrichment of phosphoryls in G3P was determined with a Agilent GC-MS operated in the selected ion-monitoring mode (357 *m/z* for ^{16}O, 359 *m/z* for $^{18}O_1$, 361 *m/z* for $^{18}O_2$, and 363 *m/z* for $^{18}O_3$) (Fig. 2c).

Electron spray ionization mass spectrometry

Purified ATP from heart extracts (^{18}O labeled and unlabeled) was 1:1 diluted with 5 mM ammonium acetate in methanol, and then infused continuously at 10 μL min^{-1} into the ion spray chamber. The system was flushed after each infusion of ATP samples with MS grade water and methanol mixture (1:1, *v*/*v*). Experiments were performed using a LTQ-Orbitrap XL MS with Tune Plus software for tuning and Xcalibur 2.0.7 software for data acquisition and processing (Thermo Fisher Scientific). The resolution of the MS was set at 30,000. The Orbitrap mass analyzer was operated with a target mass resolution of 30,000 (FWHM as defined at *m/z* 524) and a scan time of 0.3 s. Samples were analyzed using negative polarity in full scan mode. The mass spectrum from 50 to 700 *m/z* was recorded. An ATP standard (A2383 Sigma Aldrich), dissolved in MS grade water and diluted 1:1 with 5 mM ammonium acetate in methanol, was used to optimize the electrospray ionization conditions. The optimized electrospray ionization settings for ATP were a spray voltage of 4.0 kV, sheath gas at 12, Aux gas at 0, sweep gas at 2, capillary voltage at −40.0 V, capillary temperature set to 275 °C with the tube lens set at −110.0 V. Fragments at 506, 426, and 346 *m/z* and their corresponding enriched species $^{18}O_1$ (parent ion +2 *m/z*), $^{18}O_2$ (parent ion +4 *m/z*), etc., and $^{18}O_n$ (parent ion $+2\times n$ *m/z*) were analyzed.

Calculation of ^{18}O incorporation in phosphorylated compounds

The exchange of ^{16}O by ^{18}O induces a small, but measurable, chemical shift in ^{31}P NMR spectra and a 2-amu mass increase in mass spectrometry [29, 41]. This enabled direct observation

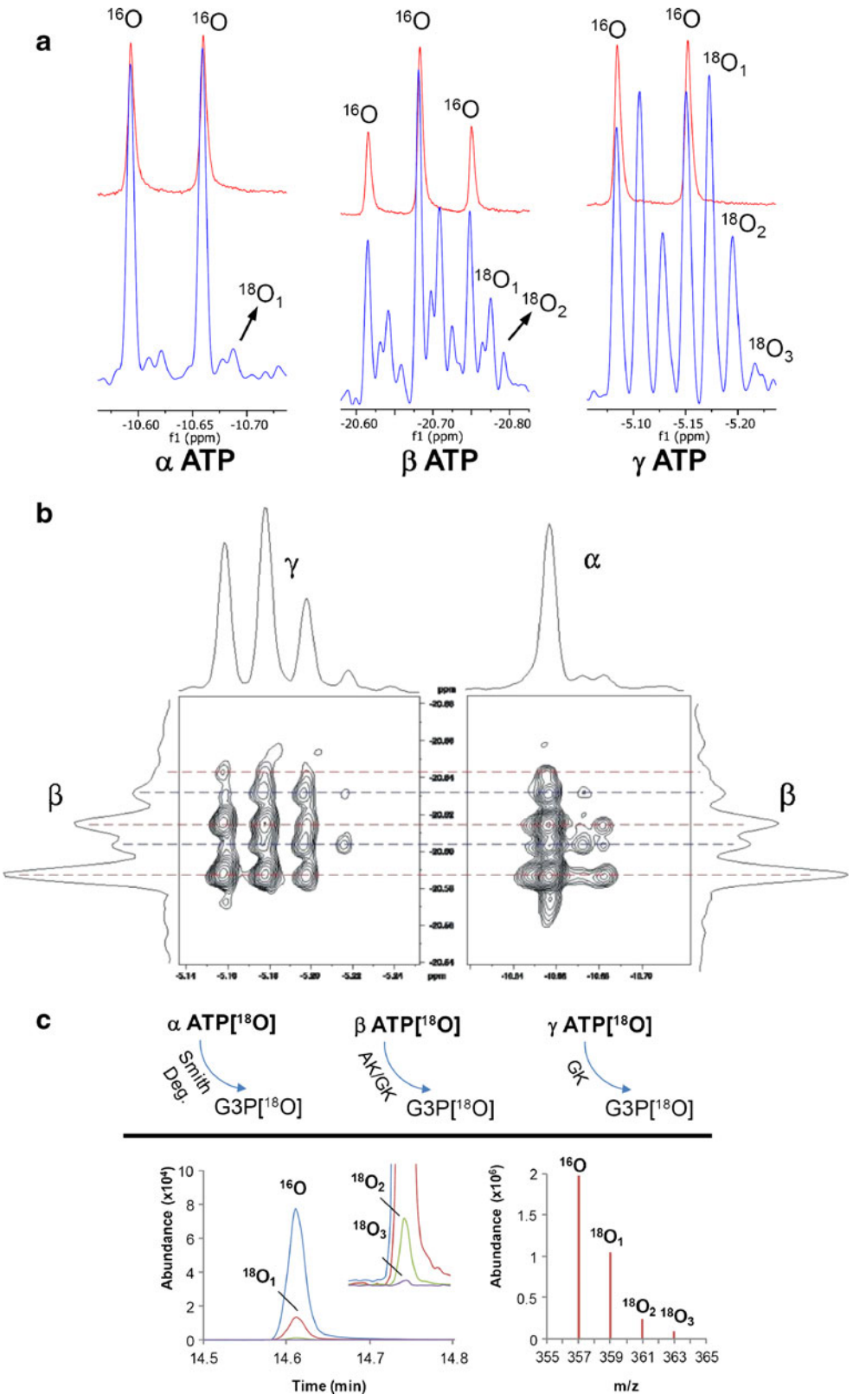

Fig. 2 Principles of methods for monitoring ^{18}O enrichment of ATP at different phosphoryl moieties. 1D ^{31}P NMR is based on ^{18}O isotope-induced shifts in α-, β-, and γ-ATP peaks (*red line*, unlabeled ATP and *blue line*, labeled ATP) (**a**). 2D ^{31}P NMR uses ^{18}O isotope-induced shifts to separate signals from all isotpologues and isotopomers (**b**). GC-MS analysis of ^{18}O-labeling of ATP α-, β- and γ-phosphoryls after Smith degradation procedure (α-) and enzymatic transfer to glycerol (β- and γ-) and subsequent measurement of ^{18}O-labeling of G3P (**c**). *AK* adenylate kinase, *GK* glycerokinase

of $^{16}O/^{18}O$ isotope exchange in phosphorylated compounds [9, 26–28, 31, 32]. The total degree of isotope exchange (p_{Tot}) was the sum of peak areas/intensities (I_k) over all exchange sites (N), weighted by the number of ^{18}O atoms in the respective

isotopologues (k), and normalized by the sum of all areas/intensities for a given ^{31}P group of lines:

$$p_{\mathrm{Tot}}\left(^{18}\mathrm{O}\right) = \frac{1}{N}\frac{\sum_{k=1}^{N} kI_k\left(^{18}\mathrm{O}\right)}{I_0\left(^{16}\mathrm{O}\right) + \sum_{k=1}^{N} I_k\left(^{18}\mathrm{O}\right)} \quad (1)$$

The cumulative percentage of ^{18}O incorporation was calculated as a ratio of the total degree of ^{18}O exchange in ATP and the total content of ^{18}O in the water used for incubation [9, 27]:

$$p_{\mathrm{Cum}}\left(^{18}\mathrm{O}\right) = \frac{p_{\mathrm{Tot}}\left(^{18}\mathrm{O}\right)}{p_{\mathrm{H_2O}}\left(^{18}\mathrm{O}\right)} \quad (2)$$

ESI-MS data simulation

Populations of ATP ^{18}O isotopologues (w_I) in the 10-oxygen site tri-phosphate were calculated (Eq. 1, reference [38]) using ^{18}O fractional enrichments of six chemically distinct oxygen groups (f_k, k ∈ αb, αp, βb, βp, γb, and γp) determined by 2D NMR spectroscopy [38]. Corresponding masses of the isotopologues (m_I) were calculated by adding the isotopic ^{18}O mass shift (δ_m=2.004) of the fractionally enriched oxygen groups as follows:

$$\begin{aligned} &m_{\mathrm{I}} = m_{\mathrm{o}} + \delta_m \sum_k f_k \\ &k = \alpha b, \alpha p, \beta b, \beta p, \gamma b, \gamma p \end{aligned} \quad (3)$$

where m_0 is mass of the ^{18}O-unlabeled ATP. Alternatively, the calculation was performed using only 3 groups of oxygen atoms (k ∈ α, β, and γb), by dropping the distinction between the bridge and peripheral oxygen atoms. The three-group fractional enrichments were determined as described in "Calculation of ^{18}O incorporation degree in phosphorylated compounds" of this section. These calculations pertain to three ATP fragmental ions which contain adenosine moieties, namely: adenosine-P_3O_{10}, adenosine-P_2O_7, and adenosine-PO_3, because they are direct descendents of the parental ATP. The only difference between P_3O_{10} and for instance P_2O_7 calculations is that from each ATP isotopologue a mass content of terminal PO_3 group is subtracted.

A stick spectrum was created by summing w_I at respective m_I. Experimental spectral shapes were simulated by convolution of the stick spectrum with a Gaussian function $e^{-\mathrm{GB}^2(m-m_I)^2}$. The Gaussian broadening (GB) values were constant for all isotopic masses of an ion, exhibiting strong dependence on ionic mass, (GB=$m^{3/2}$), i.e., GB=105 and 173 for ATP ions of 506 and 346 amu, respectively.

Results

ATP ESI-MS spectra

The ATP samples metabolically labeled with ^{18}O were obtained from hearts perfused with 30 % $H_2{}^{18}O$ in K-H solution [26, 32, 38]. After purification using HPLC, the ESI-MS spectra of unlabeled and ^{18}O-labeled ATP were recorded. To calculate the ^{18}O enrichment of phosphoryls in the ATP molecule at the α-, β-, and γ- moieties, at least three known fragments that include these phosphoryls were needed. Unlabeled ATP standards produced fragments at 78.986, 158.925, 346.054, 426.020, and 505.986 m/z that correspond to fragments indicated in Fig. 3. After choosing candidate fragments, we have optimized ATP fragmentation to increase intensity of each fragment. First we have looked at infusion solution effect on fragmentation. We were not able to get good fragmentation with MeOH:water (50:50, v/v) mixture, since there were no fragment of α-ATP (346 m/z). After that we have replaced water with a buffered solution in order to change fragmentation and also to eliminate pH changes which may occur in the sample. Using buffered solution we were able to get all fragments required for calculations, however the intensity of the fragments at 346 and 426 m/z were too low. Therefore we have applied in source fragmentation using different collision-induced dissociation (CID) and tube voltage to increase the intensity of fragments. Then we have optimized new parameters, because the more energy generally results in greater fragmentation. However, at higher energies the fragment at 506 m/z were lost. To this end, the optimal yield of selected fragments were found using a methanol 1:5-mM ammonium acetate (1:1, v/v) mixture with −100-mV tube lens voltage and −40-mV CID (Fig. 3).

The ESI-MS spectra were fitted using initial values for labeling ratios from 2D ^{31}P NMR spectra obtained from the same sample. A strong agreement between simulated and experimental spectra was obtained at fragments of 346, 426, and 506 m/z (Fig. 4). In contrast, fitting fragments at 79 (as γ-PO_3) and 159 (as γ-PO_3-β-PO_3) m/z, resulted in much larger errors which indicates that they originate from more than one position in the ATP molecule. Therefore, we focused on the fragments at 346, 426, and 506 m/z.

The ^{18}O-labeling at different positions of ATP was calculated similar to the total degree of isotope exchange (Eq. 1) but with summation over all exchangeable sites in the fragment, n:

$$p_n\left(^{18}\mathrm{O}\right) = \frac{1}{n}\frac{\sum_{k=1}^{n} kI_k\left(^{18}\mathrm{O}\right)}{I\left(^{16}\mathrm{O}\right) + \sum_{k=1}^{n} I_k\left(^{18}\mathrm{O}\right)} \quad (4)$$

Using just three main fragments with 10, 7, and 4 exchange sites (O_P atoms), with the exchange degrees, p_{506}, p_{426}, and

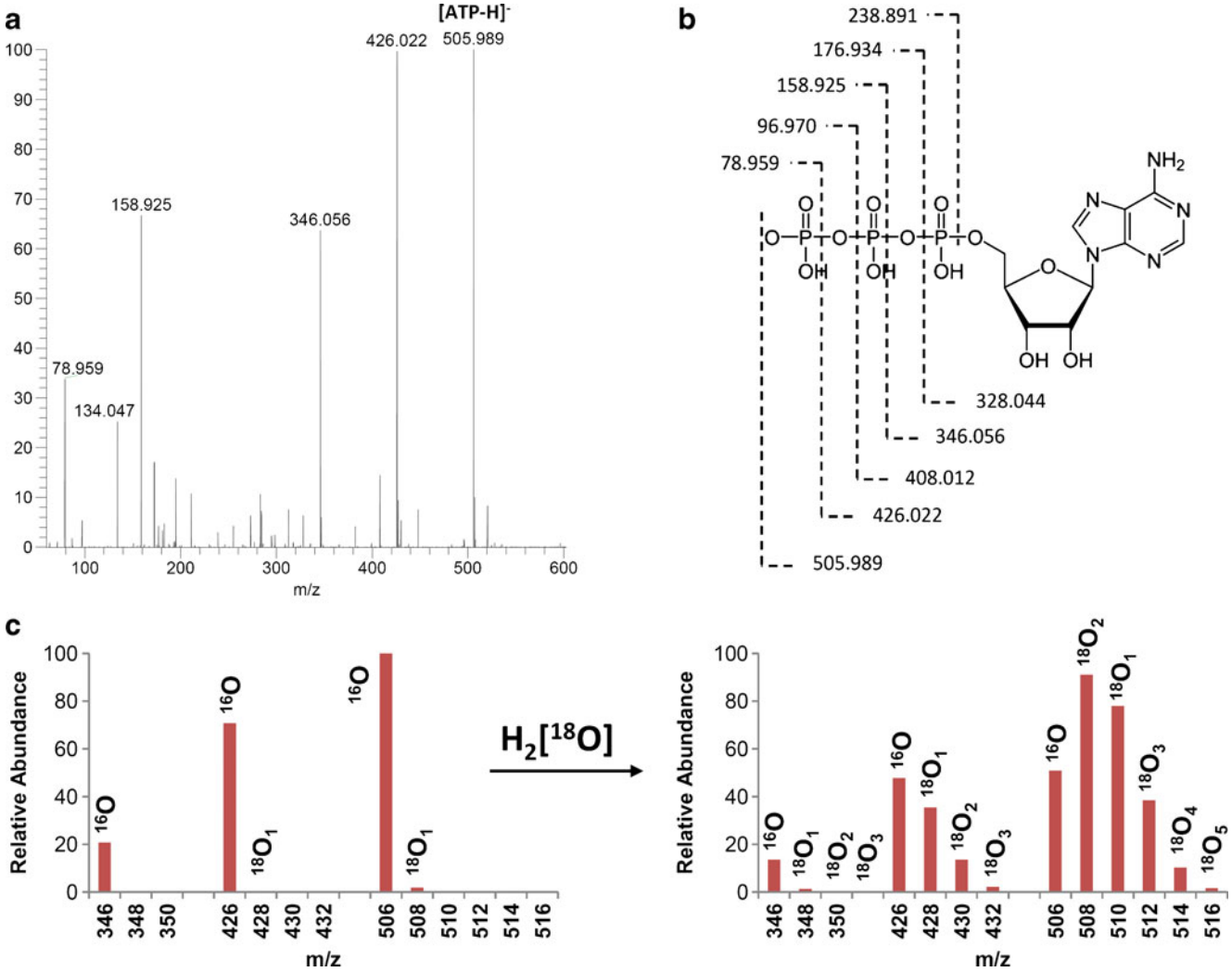

Fig. 3 Determination of ^{18}O enrichment of ATP α-, β-, and γ-phosphoryls by ESI-MS. ESI mass spectrum of ATP standard (**a**), structure and proposed MS fragmentations of ATP (**b**), and ^{18}O isotopic effects on selected MS fragments of ATP (**c**); the $^{16}O/^{18}O$ distribution spectra in phosohoryls of ATP (**c**, *left*) was obtained from unlabeled ATP extracted from rat hearts while the *right* spectra represents ^{18}O metabolically labeled ATP extracted from rat hearts

p_{346}, one obtains degrees of isotope exchange for each phosphate group:

$$\begin{aligned} p_\alpha(^{18}O) &= p_{346}(^{18}O) \\ p_\beta(^{18}O) &= \tfrac{1}{3}\left[7p_{426}(^{18}O) - 4p_{346}(^{18}O)\right] \\ p_\gamma(^{18}O) &= \tfrac{1}{3}\left[10p_{506}(^{18}O) - 7p_{426}(^{18}O)\right] \end{aligned} \quad (5)$$

In our case, Fig. 3c, $p_{346}(^{18}O)=0.027$, $p_{426}(^{18}O)=0.120$, and $p_{506}(^{18}O)=0.166$ and from Eq. 4, we found $p_\alpha=0.021$, $p_\beta=0.210$ and $p_\gamma=0.256$ which are in good agreement with enrichments obtained by NMR ($p_\alpha=0.03$, $p_\beta=0.23$, and $p_\gamma=0.25$).

To further verify the accuracy and sensitivity of ESI-MS, nine ATP samples with different ^{18}O enrichments (from mice and rat heart extracts) were analyzed with the GC-MS and ESI-MS methods. The correlation between enrichments at different phosphoryl moiety obtained by GC-MS and ESI-MS are shown in Fig. 5. The slopes were 0.98 for γ-ATP, 1.04 for β-ATP, and 2.08 for α-ATP with good linearity and regression coefficients above 0.9. We also tested the repeatability of the ESI-MS with three replicate infusions. In each case the RSD% of the whole ATP ^{18}O-labeling was lower than 0.82 z%. the concentration of ATP in samples varied with the sample origin: very high in heart tissue and very low in whole blood. Therefore, we tested the concentration effects on the labeling ratio of whole ATP. We prepared several dilutions of labeled ATP sample and found that in ESI-MS the labeling ratio became independent from a concentration above 7 nM (Fig. 5b). Thus, the optimal amount of sample for labeling ratio determination has been chosen in the middle of curve between 10 and 20 nM. This recommendation includes both reliability of measurements and sample economy considerations.

Finally, the developed method was applied to determine the turnover rates of ATP α-, β-, and γ-phosphoryls in mouse heart using the formula: $p_t(\alpha\text{-ATP})=(1-2^{-N})\times p(H_2{}^{18}O)$, where $p_t(\alpha\text{-ATP})$ is a fraction of ^{18}O-labeled α-ATP (or β- and γ-) at

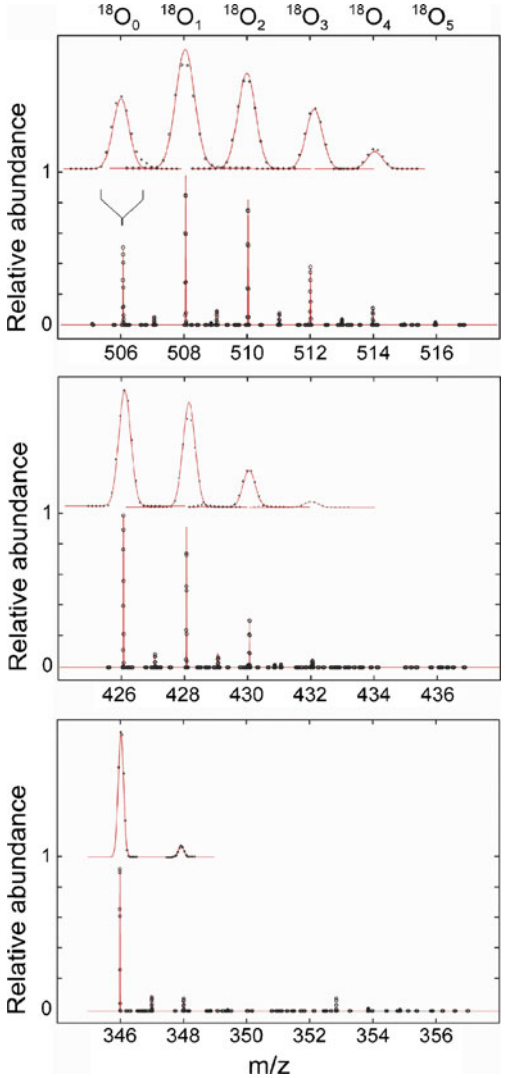

Fig. 4 Simulation of MS spectra for ATP and two fragments (less PO_4 group and less P_2O_6 group), for labeled samples. The mass distribution was calculated using fractional $^{18}O/^{16}O$ isotopic enrichments obtained by 2D NMR of the same samples. Digital (*open circles*) MS spectra of three ATP ions (from *top to bottom*, adenosine-P_3O_{10}, adenosine-P_2O_7, and adenosine-PO_3), and simulated spectral shapes obtained using three oxygen groups (*red line*)

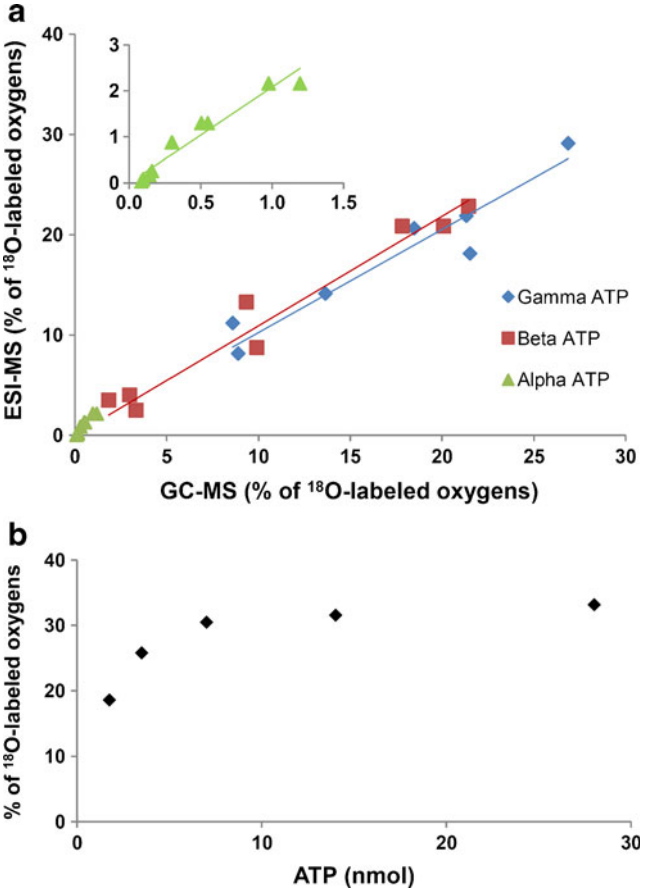

Fig. 5 Correlation of ESI-MS and GC-MS methods on γ-, β-, and α-ATP ^{18}O-labeling expressed as percent of oxygen replaced (**a**). Sample concentration effect on the accuracy of calculation of cumulative percentage of ^{18}O incorporation into ATP (**b**)

given time *t*, *N* is equal to the number of turnover cycles observed during incubation period, and $p(H_2{}^{18}O)$ is fraction of ^{18}O in media water [42–44]. In mouse hearts, ATP α-, β-, and γ-phosphoryl turnovers (*N*) were calculated to be 0.02, 0.20, and 0.57, respectively. This indicates that in mouse heart γ-ATP undergoes about 34 renewal cycles/min, β-ATP about 12 renewal cycles/min and α-ATP about 1 renewal cycle/min.

Discussion

The principal carriers of biological energy are ATP molecules containing three phosphate groups which hydrolysis are coupled with different energy consuming and biosynthetic processes in the cell [45]. In fact, the whole cellular bioenergetic system is built on sequential phosphoryl transfer reactions generating, delivering and distributing high-energy phosphoryls [46]. Cells with high-energy turnover are particularly susceptible to insults induced by lack of oxygen or metabolic substrates and their survival depend on the preservation of cellular bioenergetic system and balanced turnover rates [5, 47, 48].

Stable isotope ^{18}O-labeling is a valuable tool for monitoring turnover rates of phosphoryl-carrying metabolites and phosphotransfer network dynamics in intact tissues. The dynamics of ATP and other nucleotide triphosphate (NTP) α-, β-, and γ-phosphoryls carry on array of information regarding energetic, signal transduction and biosynthetic processes of a cell. The turnover rates of α-, β-, and γ-phosphoryls of ATP are indicators of metabolic enzyme activities, ATP turnover and phosphotransfer network dynamics in intact tissues [9, 46]. Although turnover rates of ATP at α-, β-, and γ-phosphoryl moieties have been assessed previously using radioactive and stable isotopes [43, 49–52], here we have developed method for simultaneous determination of turnover rates of three phospate moieties of ATP using ESI-MS. Advantage of such approach is in that that

it requires much smaller amount of sample (10 μL) compared with ^{31}P NMR (500 μL) and GC-MS (200 μL) and is much faster and simpler than GC-MS, with long procedures of tedious sample preparation, enzymatic and chemical reactions to clip phosphoryl moieties and derivatization. Comparing ESI-MS with other isotope labeling detection methods in oligophosphates, it is sensitive, fast, simple, and safe, especially contrasting to radioactive ^{32}P labeling studies.

A combination of NMR and MS techniques may be useful for a comprehensive evaluation of muscle and cellular bioenergetics and phosphotransfer metabolomics and fluxomics. Even partially discerned isotopologues and isotopomers in 2D ^{31}P NMR enabled accurate determination of the ^{18}O-labeling rates of NMR isotope effect-equivalent oxygen atoms within the tri-phosphoryl moiety. Consequently, the 2D method readily differentiated enrichments of the bridge and peripheral oxygen atoms. For basic analysis, this differentiation might be irrelevant but with the evidence that there are enzymes which affect these oxygen atoms differently, such a differentiation may become increasingly more relevant. Although the 2D method greatly enhanced ^{18}O-assisted ^{31}P NMR spectroscopy it is impractical for serial metabolomic studies because of low sensitivity and as it provide α/β- or β/γ-^{31}Ps correlations, one at a time. On the other hand, MS is much faster and more sensitive but, contrary to NMR the errors in the isotope enrichments for the β- and γ-sites are highly correlated. Namely, these enrichments are obtained as a weighted difference between enrichments of respective ions. Positive errors in $p_{346}(^{18}O)$ tend to increase p_β and decrease p_γ, mandating solutions. One is to find more peaks in MS with variable fragmentation (Fig. 3a) or to use a more robust method of peak fitting and simulation instead of simple algebra. Indeed, it is easy to find more MS peaks containing polyphosphate groups (P_xO_y) but enrichments obtained by their direct use are quite away from the ones found by NMR. This clearly indicates that the same fragment comes from different positions in the ATP molecule. For example, the ion P_2O_6 (158.925 *m/z*) may originate either from α-β or β-γ fragments, created by different fragmentation paths. Thus, it is impossible to use these ions directly for labeling calculation, but by taking into account the isotope enrichment known independently, e.g., from NMR, the fraction of α-β and β-γ could be calculated, and subsequently used for analysis of samples with unknown enrichment. In this way, the same fitting procedure used to analyze 2D spectra [38] could greatly improve the accuracy of the MS method. Indeed, using only three fragments that contain adenosine of ATP, the fitting procedure that includes all peak intensity simultaneously resulted in slightly different, but noticeable, differences between the peripheral and bridge beta oxygen atoms (Fig. 4). This actually means that the MS spectra are also sensitive to the isotopomer distribution. This may appear surprising at first sight, but can be accounted as different isotopomers are present in each ion with different statistical weights. We believe that a proper calibration of MS spectra, based on NMR analysis of the same sample, can ultimately enable MS to determine isotope enrichment efficiently and reliably for the bridge and peripheral oxygen atoms. Whereas a very high correlation between GC-MS and ESI-MS for γ and β labeling is observed (regression coefficients and slopes of γ- and β- enrichments close to each other), poor correlation is observed for α ATP. This could be explained by very low labeling at α-position as well as lower sensitivity and derivatization effects in GC-MS.

The possibility of $^{18}O/^{16}O$ ion exchange in the ESI source or during to sample preparation can be ignored, since the oxygen exchange between phosphate and $H_2[^{18}O]$ does not occur readily in nature [39, 40] and under ionization conditions present in ESI-MS [53]. Moreover, the possibility of gas phase ion reaction needs to be considered too. Here, the Adenosine-P_3O_{10} used in the study was purified, therefore the source of adenosine-P_2O_7 and adenosine-PO_3 was only be the adenosine-P_3O_{10} using in source fragmentation. Good correlation of LC/MS data with GC-MS and 2D ^{31}P NMR indicated that the possibility of gas phase ion reactions is negligible.

The labeling degree in ATP depends on the incubation time and the fraction of ^{18}O in the media water. However, correct calculation of the labeling degree depends on the concentration, because the signals of the fragments cannot be distinguished from noise at the low concentration even at high enrichment ratio. Therefore precautions must be given to labeling calculation. To determine correct enrichment of ATP, at least three degree of ^{18}O-labeling (the fragments at 512 *m/z*, $^{18}O_3$) must be observed. In our cases, we found that the labeling ratio becomes independent from concentration above 7 nmol (Fig. 5b) in 30 % of ^{18}O in media water for 10-min labeling.

Determined here accurate α-, β-, and γ-phosphoryl turnover rates of ATP in mouse hearts indicate that α-ATP turns over only once every minute while β- and γ-ATPs are turning over 12 and 34 cycles/min, respectively. Literature data regarding labeling and turnovers of ATP α-, β-, and γ-phosphoryls is rather sparse. In comparison, human and rat heart γ-ATP turnovers are 6 and 20 cycles/min, respectively [9, 54]. Labeling data of ATP with radioactive ^{32}P in *Escherichia coli* indicate that both β- and γ-ATPs undergo about 17 turnover cycles/min while α-ATP turns over only 1 cycle/min [51]. From similar labeling study calculated ATP turnover rates in rabbit hearts are about 25 cycles/min for β- and γ-ATPs and 0.25 cycles/min for α-ATP [43]. Thus, ESI-MS technology provides a robust and reliable method for monitoring turnover rates of phosphoryls in ATP with short analysis time and high sensitivity.

Conclusions

Knowledge of the dynamics of ATP at α-, β-, and γ-phosphoryl moieties and those in other NTPs provides valuable information about energetic and biosynthetic processes in the cell. Here, we

developed and validated the applicability of the robust ESI-MS method for determining fractional stable isotope enrichment within separate groups of mono-, di-, or tri-phosphates. The advantage of the ESI-MS over the 1D ^{31}P NMR and GC-MS was a shorter time and higher sensitivity for detection and quantification of $^{18}O/^{16}O$ exchange in individual phosphate moieties. In combination with LC, this method permits analysis of multiple mono-, di-, and tri- phosphates at the same time without any pre-purification steps. This allows simultaneous determination of almost all mono-, di-, and tri-phosphate ^{18}O-labeling ratios and turnover rates in intact tissues. Thus ESI-MS, calibrated by 2D ^{31}P NMR, provides a suitable analytical platform for dynamic phosphometabolomic profiling of tissue energy metabolism. The ESI-MS method developed here can be applied for determination of labeling ratios of other biologically important NTP (GTP, ITP, UTP, and CTP) and di-phosphates (ADP, GDP, UDP, and CDP) and inositiol oligophosphates (IP3 and IP5). Especially since concentrations of these tri-phosphates are much lower than ATP and have similar chemical shifts with ATP in ^{31}P NMR spectra. Therefore it is not possible to separate and determine ^{18}O-labeling of other NTPs in the presence of ATP using ^{31}P NMR. Thus, ESI-MS method can be applied to analyze ^{18}O-labeling and turnover of multiple oligophosphates at very low concentration in biological samples.

Acknowledgments We would like to thank Mai T. Persson, Godfrey C. Ford, and Linda M. Benson for their technical assistance with ESI-MS analyses. This work has been supported by NIH, Marriott Heart Disease Research Program, Marriott Foundation, and Mayo Clinic. This work was supported by NIH/NCRR CTSA grant number UL1 RR024150.

References

1. Saks V, Dzeja P, Schlattner U, Vendelin M, Terzic A, Wallimann T (2006) Cardiac system bioenergetics: metabolic basis of the Frank–Starling law. J Physiol-London 571(2):253–273. doi:10.1113/jphysiol.2005.101444
2. Arrell DK, Terzic A (2010) Network systems biology for drug discovery. Clin Pharmacol Ther 88(1):120–125. doi:10.1038/Clpt.2010.91
3. Dzeja PP, Chung S, Faustino RS, Behfar A, Terzic A (2011) Developmental enhancement of adenylate kinase-AMPK metabolic signaling axis supports stem cell cardiac differentiation. PLoS One 6 (4):10.1371/journal.pone.0019300
4. Dzeja PP, Bortolon R, Perez-Terzic C, Holmuhamedov EL, Terzic A (2002) Energetic communication between mitochondria and nucleus directed by catalyzed phosphotransfer. Proc Natl Acad Sci U S A 99(15):10156–10161. doi:10.1073/pnas.152259999
5. Dzeja PP, Hoyer K, Tian R, Zhang S, Nemutlu E, Spindler M, Ingwall JS (2011) Rearrangement of energetic and substrate utilization networks compensate for chronic myocardial creatine kinase deficiency. J Physiol-London 589(21):5193–5211. doi:10.1113/jphysiol.2011.212829
6. Janssen E, Terzic A, Wieringa B, Dzeja PP (2003) Impaired intracellular energetic communication in muscles from creatine kinase and adenylate kinase (M-CK/AK1) double knock-out mice. J Biol Chem 278(33):30441–30449. doi:10.1074/jbc.M303150200
7. Dzeja P, Terzic A (2009) Adenylate kinase and AMP signaling networks: metabolic monitoring, signal communication and body energy sensing. Int J Mol Sci 10(4):1729–1772. doi:10.3390/Ijms10041729
8. Janssen E, de Groof A, Wijers M, Fransen J, Dzeja PP, Terzic A, Wieringa B (2003) Adenylate kinase 1 deficiency induces molecular and structural adaptations to support muscle energy metabolism. J Biol Chem 278(15):12937–12945. doi:10.1074/jbc.M211465200
9. Pucar D, Dzeja PP, Bast P, Juranic N, Macura S, Terzic A (2001) Cellular energetics in the preconditioned state—protective role for phosphotransfer reactions captured by ^{18}O-assisted ^{31}P NMR. J Biol Chem 276(48):44812–44819
10. Vincent G, Khairallah M, Bouchard B, Des Rosiers C (2003) Metabolic phenotyping of the diseased rat heart using ^{13}C-substrates and ex vivo perfusion in the working mode. Mol Cell Biochem 242(1–2):89–99
11. Li W, Bian F, Chaudhuri P, Mao XA, Brunengraber H, Yu X (2011) Delineation of substrate selection and anaplerosis in tricarboxylic acid cycle of the heart by ^{13}C NMR spectroscopy and mass spectrometry. NMR Biomed 24(2):176–187. doi:10.1002/Nbm.1569
12. Pound KM, Sorokina N, Ballal K, Berkich DA, Fasano M, LaNoue KF, Taegtmeyer H, O'Donnell JM, Lewandowski ED (2009) Substrate-enzyme competition attenuates upregulated anaplerotic flux through malic enzyme in hypertrophied rat heart and restores triacylglyceride content attenuating upregulated anaplerosis in hypertrophy. Circ Res 104(6):805–812. doi:10.1161/Circresaha.108.189951
13. Kruger NJ, Ratcliffe RG (2009) Insights into plant metabolic networks from steady-state metabolic flux analysis. Biochimie 91(6):697–702. doi:10.1016/j.biochi.2009.01.004
14. Paul Lee WN, Wahjudi PN, Xu J, Go VL (2010) Tracer-based metabolomics: concepts and practices. Clin Biochem 43(16–17):1269–1277
15. Janssen E, Dzeja PP, Oerlemans F, Simonetti AW, Heerschap A, de Haan A, Rush PS, Terjung RR, Wieringa B, Terzic A (2000) Adenylate kinase 1 gene deletion disrupts muscle energetic economy despite metabolic rearrangement. EMBO J 19(23):6371–6381. doi:10.1093/emboj/19.23.6371
16. Griffin JL, Des Rosiers C (2009) Applications of metabolomics and proteomics to the mdx mouse model of Duchenne muscular dystrophy: lessons from downstream of the transcriptome. Genome Med 1(3):1–11
17. Kelleher JK (2001) Flux estimation using isotopic tracers: common ground for metabolic physiology and metabolic engineering. Metab Eng 3(2):100–110
18. Tang Y, Pingitore F, Mukhopadhyay A, Phan R, Hazen TC, Keasling JD (2007) Pathway confirmation and flux analysis of central metabolic pathways in Desulfovibrio vulgaris Hildenborough using gas chromatography-mass spectrometry and Fourier transform-ion cyclotron resonance mass spectrometry. J Bacteriol 189(3):940–949. doi:10.1128/Jb.00948-06
19. Zamboni N (2011) ^{13}C metabolic flux analysis in complex systems. Curr Opin Biotechnol 22(1):103–108. doi:10.1016/j.copbio.2010.08.009
20. Lee WNP, Wahjudi PN, Xu J, Go VL (2010) Tracer-based metabolomics: concepts and practices. Clin Biochem 43(16–17):1269–1277. doi:10.1016/j.clinbiochem.2010.07.027
21. Lane AN, Fan TWM, Higashi RM (2008) Isotopomer-based metabolomic analysis by NMR and mass spectrometry. Methods Cell Biol 84:541–588. doi:10.1016/S0091-679x(07)84018-0, Biophysical Tools for Biologists: Vol 1 in Vitro Techniques
22. Sauer U (2006) Metabolic networks in motion: C-13-based flux analysis. Mol Syst Biol 2. doi:10.1038/Msb4100109
23. Zeleznikar RJ, Goldberg ND (1991) Kinetics and compartmentation of energy metabolism in intact skeletal muscle determined from ^{18}O labeling of metabolite phosphoryls. J Biol Chem 266 (23):15110–15119

24. Malloy CR, Merritt ME, Dean Sherry A (2011) Could ^{13}C MRI assist clinical decision-making for patients with heart disease? NMR Biomed 24(8):973–979
25. Stempel KE, Boyer PD (1986) Refinement in oxygen-18 methodology for the study of phosphorylation mechanisms. Methods Enzymol 126:618–639
26. Pucar D, Janssen E, Dzeja PP, Juranic N, Macura S, Wieringa B, Terzic A (2000) Compromised energetics in the adenylate kinase AK1 gene knockout heart under metabolic stress. J Biol Chem 275 (52):41424–41429. doi:10.1074/jbc.M007903200
27. Pucar D, Dzeja PP, Bast P, Gumina RJ, Drahl C, Lim L, Juranic N, Macura S, Terzic A (2004) Mapping hypoxia-induced bioenergetic rearrangements and metabolic signaling by ^{18}O-assisted ^{31}P NMR and ^{1}H NMR spectroscopy. Mol Cell Biochem 256(1–2):281–289
28. Pucar D, Bast P, Gumina RJ, Lim L, Drahl C, Juranic N, Macura S, Janssen E, Wieringa B, Terzic A, Dzeja PP (2002) Adenylate kinase AK1 knockout heart: energetics and functional performance under ischemia-reperfusion. Am J Physiol Heart Circ Physiol 283 (2):H776–782. doi:10.1152/ajpheart.00116.2002
29. Cohn M, Hu A (1978) Isotopic (^{18}O) shift in ^{31}P nuclear magnetic resonance applied to a study of enzyme-catalyzed phosphate–phosphate exchange and phosphate (oxygen)–water exchange reactions. Proc Natl Acad Sci U S A 75(1):200–203
30. Zeleznikar RJ, Dzeja PP, Goldberg ND (1995) Adenylate kinase-catalyzed phosphoryl transfer couples ATP utilization with its generation by glycolysis in intact muscle. J Biol Chem 270(13):7311–7319
31. Dzeja PP, Zeleznikar RJ, Goldberg ND (1996) Suppression of creatine kinase-catalyzed phosphotransfer results in increased phosphoryl transfer by adenylate kinase in intact skeletal muscle. J Biol Chem 271(22):12847–12851
32. Dzeja PP, Vitkevicius KT, Redfield MM, Burnett JC, Terzic A (1999) Adenylate kinase-catalyzed phosphotransfer in the myocardium—increased contribution in heart failure. Circ Res 84(10):1137–1143
33. Westheimer FH (1987) Why nature chose phosphates. Science 235 (4793):1173–1178
34. Dawis SM, Walseth TF, Deeg MA, Heyman RA, Graeff RM, Goldberg ND (1989) Adenosine triphosphate utilization rates and metabolic pool sizes in intact cells measured by transfer of ^{18}O from water. Biophys J 55(1):79–99. doi:10.1016/S0006-3495(89)82782-1
35. Zeleznikar RJ, Heyman RA, Graeff RM, Walseth TF, Dawis SM, Butz EA, Goldberg ND (1990) Evidence for compartmentalized adenylate kinase catalysis serving a high energy phosphoryl transfer function in rat skeletal muscle. J Biol Chem 265(1):300–311
36. Knowles JR (1980) Enzyme-catalyzed phosphoryl transfer reactions. Annu Rev Biochem 49:877–919. doi:10.1146/annurev.bi.49.070180.004305
37. Weber DJ, Bhatnagar SK, Bullions LC, Bessman MJ, Mildvan AS (1992) NMR and isotopic exchange studies of the site of bond cleavage in the MutT reaction. J Biol Chem 267(24):16939–16942
38. Juranic N, Nemutlu E, Zhang S, Dzeja P, Terzic A, Macura S (2011) ^{31}P NMR correlation maps of $^{18}O/^{16}O$ chemical shift isotopic effects for phosphometabolite labeling studies. J Biomol NMR 50(3):237–245. doi:10.1007/s10858-011-9515-3
39. Blake RE, ONeil JR, Garcia GA (1997) Oxygen isotope systematics of biologically mediated reactions of phosphate.1. Microbial degradation of organophosphorus compounds. Geochim Et Cosmochim Acta 20:4411–4422
40. Kolodny Y, Luz B, Navon O (1983) Oxygen isotope variations in phosphate of biogenic apatites. 1. Fish bone apatite—rechecking the rules of the game. Earth Planet Sci Lett 64(3):398–404
41. Cohn M, Hu A (1980) Isotopic ^{18}O shifts in ^{31}P NMR of adenosine nucleotides synthesized with ^{18}O in various positions. J Am Chem Soc 103:913–916
42. Karl DM, Bossard P (1985) Measurement of microbial nucleic acid synthesis and specific growth rate by PO_4 and [H]adenine: field comparison. Appl Environ Microbiol 50(3):706–709
43. Rossi A (1975) ^{32}P labelling of the nucleotides in alpha-position in the rabbit heart. J Mol Cell Cardiol 7(12):891–906
44. Zilversmit DB, Entenman C, Fishler MC (1943) On the calculation of "turnover time" and "turnover rate" from experiments involving the use of labeling agents. J Gen Physiol 26(3):325–331
45. Ingwall JS (2002) ATP and the heart, vol 11. Kluwer, Norwell
46. Dzeja PP, Terzic A (2003) Phosphotransfer networks and cellular energetics. J Exp Biol 206(12):2039–2047. doi:10.1242/Jeb.00426
47. Xiong QA, Du F, Zhu XH, Zhang PY, Suntharalingam P, Ippolito J, Kamdar FD, Chen W, Zhang JY (2011) ATP production rate via creatine kinase or ATP synthase in vivo a novel superfast magnetization saturation transfer method. Circ Res 108(6):653–U265. doi:10.1161/Circresaha.110.231456
48. Ingwall JS, Shen WQ (2010) On energy circuits in the failing myocardium. Eur J Hear Fail 12(12):1268–1270. doi:10.1093/eurjhf/hfq193
49. Levinson C, Gordon ED Jr (1971) Phosphorus incorporation in the Ehrlich ascites tumor cell. J Cell Physiol 78(2):257–264. doi:10.1002/jcp.1040780213
50. Karl DM, Bossard P (1985) Measurement and significance of ATP and adenine nucleotide pool turnover in microbial cells and environmental samples. J Microbiol Methods 3(3–4):125–139
51. Lutkenhaus J, Ryan J, Konrad M (1973) Kinetics of phosphate incorporation into adenosine triphosphate and guanosine triphosphate in bacteria. J Bacteriol 116(3):1113–1123
52. Zahn D, Klinger R, Frunder H (1969) Enzymic flux rates within the mononucleotides of the mouse liver. Eur J Biochem 11(3):549–553
53. Alvarez R, Evans LA, Milham P, Wilson MA (2000) Analysis of oxygen-18 in orthophosphate by electrospray ionisation mass spectrometry. Int J Mass Spectrom 203(1–3):177–186
54. Opie LH, Opie L (1998) The heart: physiology, from cell to circulation. Lippincott-Raven, Philadelphia